Published OnlineFirst October 1, 2014; DOI: 10.1158/0008-5472.CAN-14-0914

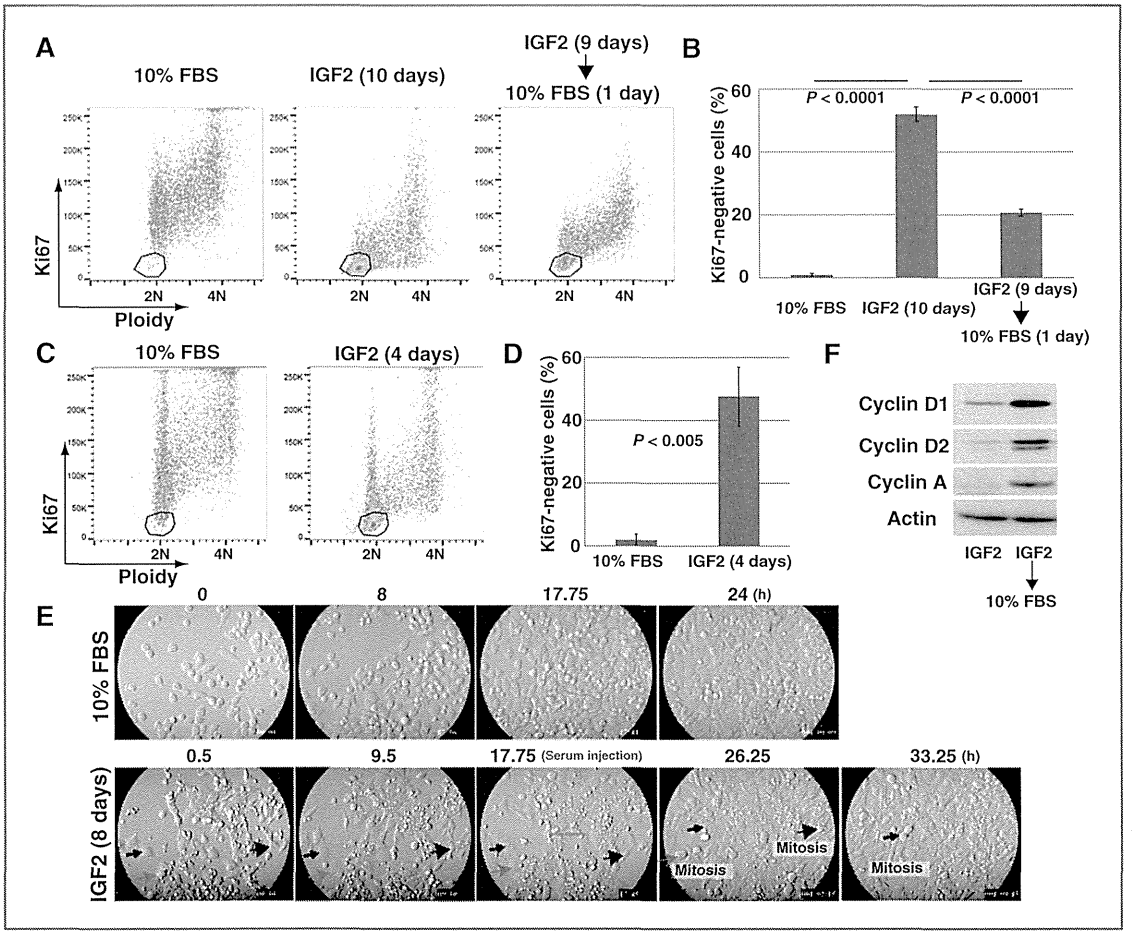

Figure 2. Dormancy-like state induced under the presence of IGF2. A, representative flow cytometric analysis of AXT cells maintained in serum-containing medium, cultured in IGF2-containing medium for 10 days, or exposed to IGF2 for 9 days and then to serum for 1 day. Ki67-negative population is enclosed by a polygon. B, quantitation of the Ki67-negative population for cells analyzed as in A. C, representative flow cytometric analysis of SAOS2 cells maintained in serum-containing medium or cultured in IGF2-containing medium for 4 days. D, quantitation of the Ki67-negative population for cells analyzed as in C. E, time-lapse video microscopy of AXT cell proliferation at the indicated times for cells either maintained in the presence of serum (top) or cultured with IGF2 for 8 days (bottom). Representative cells traced until mitosis are indicated by arrows. F, immunoblot analysis of cyclin expression in AXT cells cultured with IGF2 for 7 days or with IGF2 for 6 days and then with serum for 1 day.

similar results with the human osteosarcoma cell lines SAOS2 and U2OS (Fig. 3D and E). A low level of signal activation was still apparent in AXT cells exposed to IGF2 or insulin for 7 days. Inhibition of Akt activity resulted in the decrease of cell viability to a greater extent than in the presence of serum, suggesting that this low level of activation is critical to support cell survival (Supplementary Fig. S3A). IGF1R appeared to be constitutively activated in AXT cells cultured in the presence of IGF2 (Supplementary Fig. S3B). These findings suggested that the dormancy-like state elicited by continuous exposure of osteosarcoma cells to IGF2 is partially attributable to downregulation of survival signaling caused by attenuation of responsiveness of IGF1R signaling pathways to IGF2.

Dormancy-like state confers resistance to anticancer drugs

Given that slowly cycling cells are resistant to anticancer agents (16), we examined whether the dormancy-like state alters the sensitivity of osteosarcoma cells to such agents. Whereas exposure of AXT cells to IGF2 in the presence of serum did not affect the sensitivity of the cells to adriamycin, that in the absence of serum reduced the sensitivity compared with that apparent in the presence of serum (Fig. 4A and B). The same reduction of sensitivity could also be observed concerning cisplatin and methotrexate. Treatment of AXT cells with insulin conferred a similar level of drug resistance (Fig. 4C and Supplementary Fig. S4A and S4B). Similar results were also obtained with the human

Published OnlineFirst October 1, 2014; DOI: 10.1158/0008-5472.CAN-14-0914

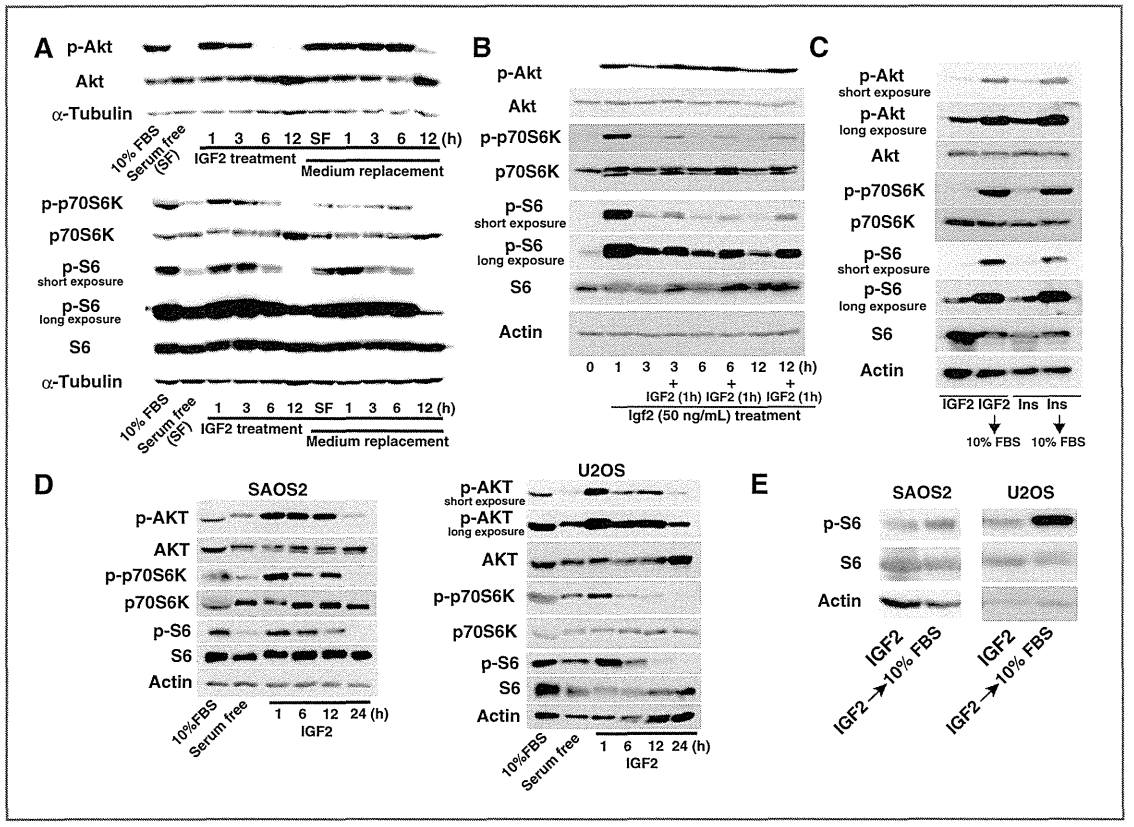

Figure 3. Immunoblot analysis of signaling molecules downstream of IGF1R. A, AXT cells were either maintained in serum-containing medium or deprived of serum for 2 hours and then exposed to IGF2 for the indicated times either without or with medium replenishment for the final 30 minutes of incubation. B, AXT cells were cultured with IGF2 for 3 days and then exposed to IGF2 for the indicated times. The 0 hour indicates 24 hours after the final medium replacement. Cells were also subjected to medium replenishment at 3, 6, and 12 hours and incubation for 1 hour before protein collection. C, AXT cells were either cultured with IGF2 or insulin (Ins) for 7 days or exposed to IGF2 or insulin for 6 days and then incubated with serum for 1 day. D, SAOS2 or U2OS cells were either maintained in serum-containing medium or deprived of serum for 3 hours and then exposed to IGF2 for the indicated times. E, SAOS2 or U2OS cells were either cultured with IGF2 for 10 or 6 days, respectively, or exposed to IGF2 for 9 or 5 days and then incubated with serum for 1 day.

osteosarcoma cell lines SAOS2 and U2OS exposed to IGF2 (Fig. 4D).

To elucidate the mechanisms responsible for the reduced sensitivity, we examined the amount of phosphorylated histone H2AX (γH2AX), a marker of DNA damage (17, 18). The proportion of AXT cells found to be highly positive for γH2AX increased to 65.7% and 52.4% after treatment with adriamycin or cisplatin, respectively, in serum-containing medium. In contrast, the corresponding values for cells cultured in the presence of IGF2 were only 38.6% and 31.5%, respectively. Conversely, the proportion of γH2AX-negative cells was higher for AXT cells cultured with IGF2 than for those cultured with serum (Fig. 4E and Supplementary Fig. S4C and S4D). In addition, we found significant upregulation of Gsts and their enzymatic activity (Fig. 4F and G), suggesting that detoxication process is enhanced under IGF2-mediated dormancy-like state compared with in the presence of serum (19).

These findings suggested that the dormancy-like state of osteosarcoma cells by long-term exposure to IGF2 renders the cells resistant to cytotoxicity induced by chemotherapeutic drugs.

Survival in IGF2 medium is dependent on glutamine and autophagy

To gain further insight into the mechanism underlying the dormancy-like state, we examined the effects of various agents. Consequently, those related to glutamine metabolism or autophagy showed similar or greater cytotoxic effects on AXT cells cultured in the presence of IGF2 or insulin than on those maintained in the presence of serum (Fig. 5A and B and Supplementary Fig. S5), implicating these processes in the dormancy-like state. Depletion of glutamine from IGF2- or insulin-containing medium resulted in total suppression of AXT cell survival (Fig. 5C).

The conversion of LC3I to LC3II is indicative of an increase in autophagy flux (20, 21). The accumulation of LC3II in AXT cells cultured in the presence of serum suggests the constitutive activation of autophagy. The ratio of LC3II to LC3I appeared

Published OnlineFirst October 1, 2014; DOI: 10.1158/0008-5472.CAN-14-0914

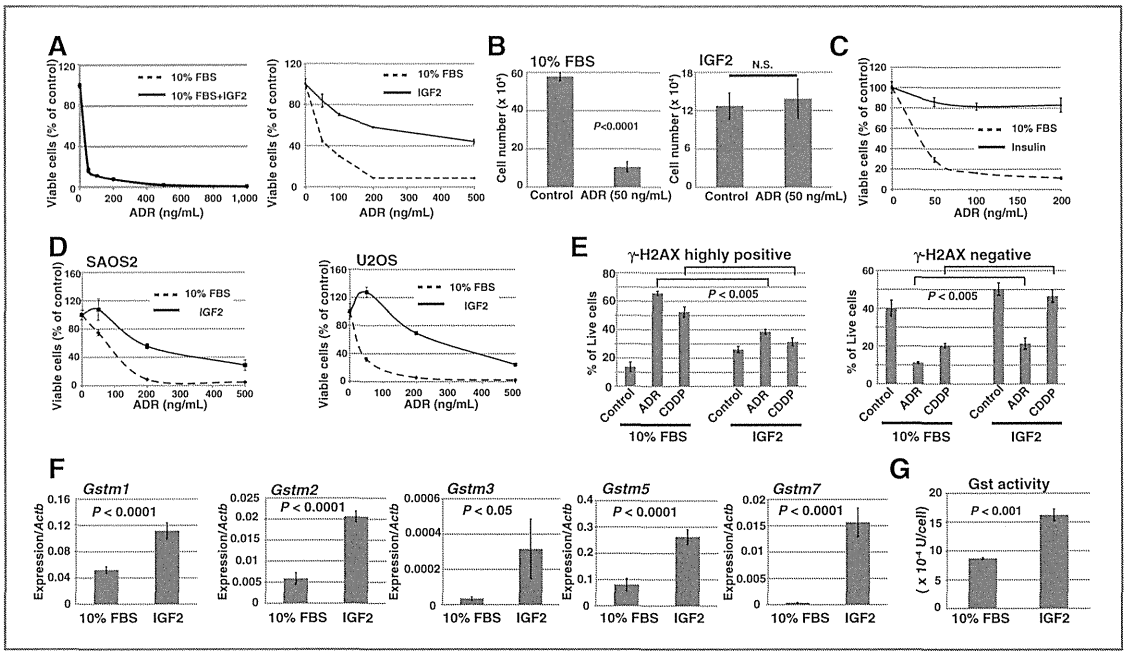

Figure 4. Long-term exposure of osteosarcoma cells to IGF2 confers resistance to anticancer drugs. A, viable AXT cells were assessed after exposure for 2 days to the indicated concentrations of adriamycin (ADR) in medium containing serum or both serum and IGF2 (left) or in medium containing serum or IGF2 (right). B, number of viable AXT cells evaluated by trypan blue exclusion was counted after exposure to adriamycin for 2 days in medium containing serum or IGF2. C, viable AXT cells were assessed after exposure for 2 days to the indicated concentrations of adriamycin in medium containing serum or insulin. D, viable SAOS2 or U2OS cells were evaluated after exposure for 2 days to the indicated concentrations of adriamycin in medium containing serum or IGF2. E, quantitation of AXT cells highly positive or negative for γH2AX evaluated by flow cytometric analyses after culture in the presence of serum or IGF2 for 7 days and then incubated in the additional presence of adriamycin (100 ng/mL) or cisplatin (CDDP; 100 ng/mL) for 24 hours. F, real-time PCR analysis of *Gstm* expression in AXT cells cultured in the presence of serum or IGF2-containing medium for 6 days. G, Gst activity of AXT cells cultured in the presence of serum or IGF2-containing medium for 5 days.

even greater in AXT cells maintained in IGF2-containing medium than in those cultured in the presence of serum (Fig. 5D), suggestive of a more pronounced increase in autophagy flux. Treatment of chloroquine resulted in the accumulation of LC3II by blocking autophagy in its final step (22). Electron microscopy revealed the presence of a greater number of vacuoles, including autophagosomes with a double-membrane structure, in the cytoplasm of AXT cells cultured with IGF2 compared with those maintained in the presence of serum (Fig. 5E). Consistent with these findings, knockdown of Atg7, an E1-like enzyme required for autophagy (21, 23), not only reduced the abundance of LC3II (suggestive of inhibition of autophagy; Fig. 5F) but also attenuated the viability of AXT cells maintained in the presence of IGF2 or insulin (Fig. 5G and H). Thus, the maintenance of osteosarcoma cell survival by IGF2 or insulin appears to be dependent on enhancement of autophagy.

Suppression of autophagy and depletion of glutamine enhance the antitumor activity of chemotherapeutic agents *in vivo*

We investigated whether the suppression of autophagy flux or depletion of glutamine might have an antitumor effect *in vivo*. Chloroquine, bafilomycin A, or L-asparaginase enhanced the antitumor activity of the combination of adriamycin, ifosfamide, and methotrexate (Fig. 6A). Treatment with L-asparaginase, which hydrolyzes asparagine and glutamine to produce aspartate and glutamate, respectively (24), reduced the serum concentration of glutamine and increased those of glutamate and aspartate (Supplementary Fig. S6A). The chemotherapeutic drugs alone increased the expression of LC3 in some tumors (Fig. 6B and C), suggesting that autophagy flux could be increased by chemotherapy. Additional treatment with chloroquine or bafilomycin A had a more pronounced effect on LC3 accumulation in tumors than in chemotherapy alone (Fig. 6B and C), likely reflecting the effective inhibition of autophagy (22). Combined treatment with chemotherapy and these agents not only resulted in a reduction in tumor size but also induced severe damage to osteosarcoma cells and a consequent loss of solidity within tumors compared with the effects of chemotherapy alone (Fig. 6C and Supplementary Fig. S6B). Collectively, these findings suggested that a combination of agents targeted to the dormancy-like cells and conventional chemotherapy is a potential therapeutic option for osteosarcoma.

Increased expression levels of IGFs after chemotherapy in human osteosarcoma

We finally analyzed seven paired pre- and postchemotherapy human osteosarcoma samples to examine the correlation

Published OnlineFirst October 1, 2014; DOI: 10.1158/0008-5472.CAN-14-0914

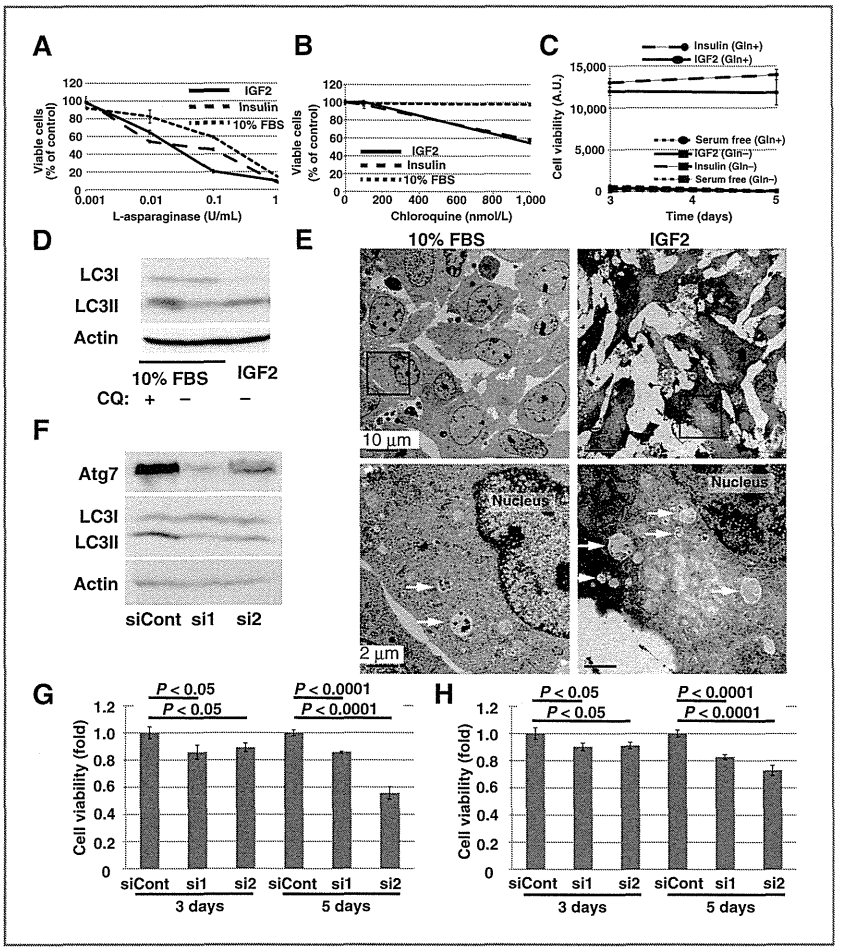

Figure 5. Survival in the dormancy-like state is dependent on glutamine and autophagy. A and B, viability of AXT cells was assessed after exposure for 2 days to the indicated concentrations of L-asparaginase or chloroquine in medium containing IGF2, insulin, or serum. C, viability of AXT cells was assayed at the indicated times after culture in the absence or presence of IGF2 or insulin and with or without glutamine. Data are presented in arbitrary units (A.U.). D, immunoblot analysis of LC3 in AXT cells cultured in the presence of serum or IGF2 for 12 days. Cells were also exposed to 50 μmol/L chloroquine (CQ) for the final 24 hours before analysis for the indication of LC3II. E, representative electron microscopy of AXT cells cultured in the presence of serum or IGF2 for 12 days. The boxed areas in the top are shown at higher magnification in the bottom. Arrows, vacuoles. F, immunoblot analysis of Atg7 and LC3 in AXT cells at 4 days after transfection with control (siCont) or Atg7-targeted (si1, si2) siRNAs. G and H, viable AXT cells transfected with each siRNA were assessed after culture in the presence of IGF2 (G) or insulin (H) for 3 or 5 days. Assays were performed in quadruplicate, and each ratio relative to the value for day 0 was calculated.

between the expression levels of IGFs and chemotherapy (Fig. 6D and Table 1). *IGF1* expression tends to be upregulated after chemotherapy in all tumor samples. In contrast, *IGF2* expression basically varied between samples and both downregulation and upregulation were observed after chemotherapy. However, notably, in OS-1, 2, 4, 5, and 6 with favorable prognosis, *IGF2* level was decreased after chemotherapy, otherwise the cases (OS-3, 7) did not achieve successful clinical course. In addition, a case (OS-7) whose expression level of *IGF2* was markedly upregulated after chemotherapy exhibited poor response to chemotherapy.

Discussion

We have here shown that the expression level of *Igf2* was elevated in osteosarcoma cells damaged by chemotherapy. Although serum-free condition induced cell death, presence of IGF2 or insulin could guarantee survival of AXT cells, which, consequently, caused dormancy-like state, as evidenced by reduced expression of Ki67, downregulation of cyclins, and decreased activation level of survival signaling. Importantly, subsequent exposure to serum released the cells from the dormancy-like state.

Components of the microenvironment have increasingly been implicated in the maintenance of normal tissue stem cells in a dormant state (25, 26). AXT cells were established from bone marrow stromal cells of *Ink4a/Arf* knockout mice and harbor a mutant form (R267C) of p53 (data not shown). Although the stress-activated protein kinase p38 or changes in the activity of related signaling molecules have been suggested to regulate quiescence in cancer cells (27, 28), the mechanisms underlying the induction of quiescence in the cells whose machinery for arresting cell cycle is almost impaired like AXT remain to be elucidated.

Growth factor signaling networks incorporate negative feedback system to maintain homeostasis (29). Previous reports suggest that activation of the IGF/insulin signaling is limited by feedback inhibition, which is mediated by the PI3K–AKT–mTOR pathway. Activated S6K phosphorylates IRS proteins, which induces degradation of IRS proteins,

Published OnlineFirst October 1, 2014; DOI: 10.1158/0008-5472.CAN-14-0914

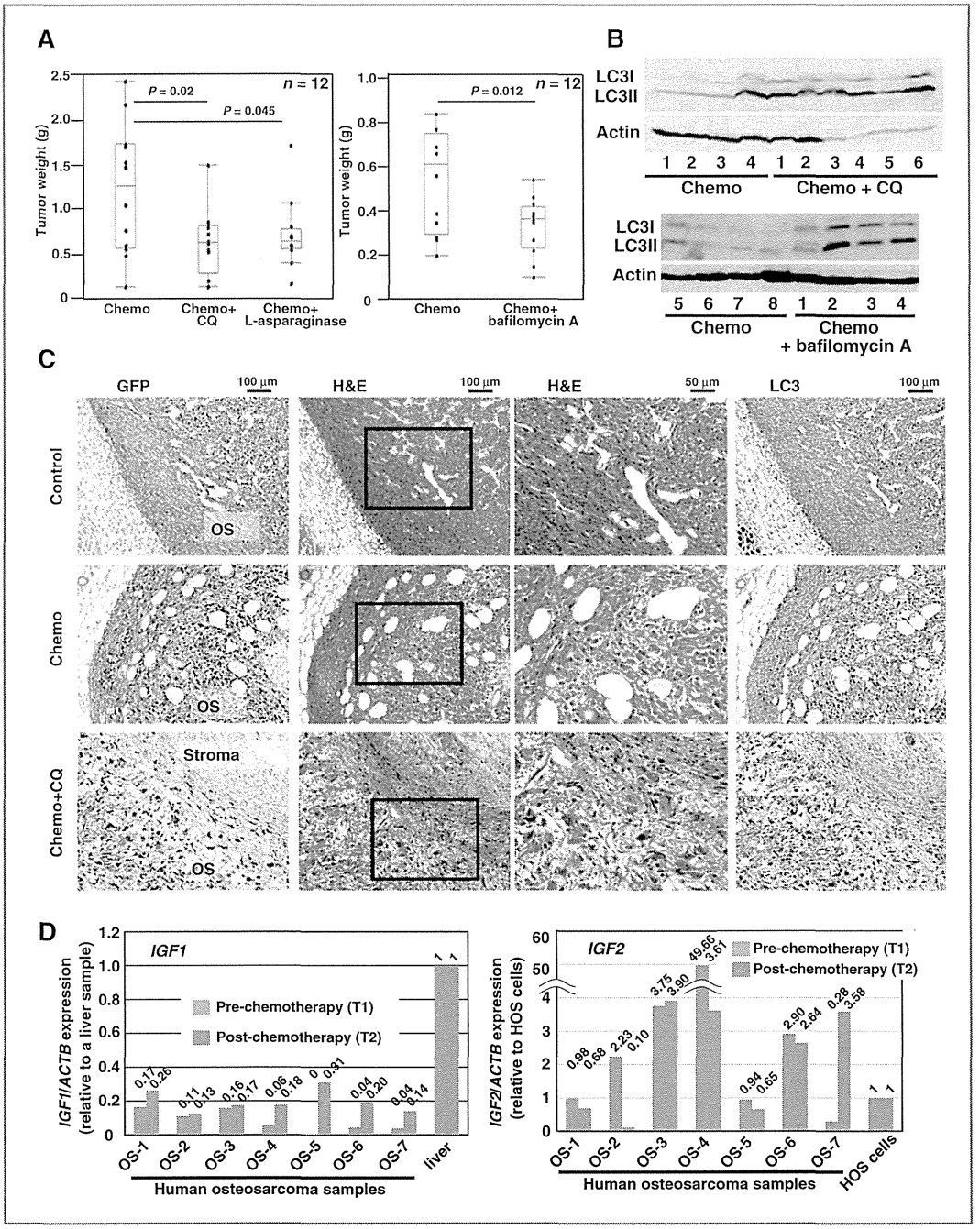

Figure 6. Chloroquine, bafilomycin A and L-asparaginase enhance antitumor activity of conventional chemotherapy *in vivo*. A, weight of AXT cell–derived tumors for mice subjected to chemotherapy (Chemo) either alone or together with chloroquine (CQ), L-asparaginase, or bafilomycin A. Data are presented as box-and-whisker plots for 12 tumors. B, immunoblot analysis of LC3 in individual tumors treated with chemotherapy either alone or together with chloroquine or bafilomycin A as in A. Numbers indicate the individual tumor. C, serial sections of tumors from mice treated with chemotherapy either alone or together with chloroquine as in A were subjected both to hematoxylin and eosin (H&E) staining and to immunohistochemical analysis for GFP and LC3. Boxed regions in the H&E on the left are shown at higher magnification in the corresponding panels on the right. D, real-time PCR analysis of *IGF1* and *2* expressions in paired pre- (blue) and post- (orange) chemotherapy human osteosarcoma samples. Values relative to respective positive control (a liver sample or HOS cells) are also shown.

Published OnlineFirst October 1, 2014; DOI: 10.1158/0008-5472.CAN-14-0914

Table 1. Characteristics of human patients with osteosarcoma

ID	Age, y	Metastasis	Gender	Location	Follow-up, mo	Final status
OS-1	20	(-)	Male	Tibia	132	CDF
OS-2	6	(-)	Female	Fibula	126	CDF
OS-3	20	Lung	Male	Tibia	42	DOD
OS-4	17	(-)	Male	Tibia	116	CDF
OS-5	15	(-)	Male	Femur	95	CDF
OS-6	22	(-)	Male	Femur	89	CDF
OS-7	15	(-)	Female	Femur	31	DOD

Abbreviations: CDF, continuously disease-free; DOD, died of disease.

reduction of their interaction with IGF1R and insulin receptor, or the inhibition of their downstream signaling. Negative feedback from downstream effectors has also been implicated in the insulin resistance that results in impaired glucose tolerance in diabetes (30–32). Similar negative feedback might contribute to the dormant osteosarcoma cells under continuous exposure to IGF2 or insulin. The constitutive activation of IGF1R in AXT cells exposed to IGF2 might partially support this notion.

A very recent report suggests the direct implication of IGF2 in the emergence of therapeutic resistance in cancer (33). Overexpression of IGFs and IGFRs is commonly observed in human osteosarcoma and is implicated in disease pathogenesis (34–37). Because of the difficulty in obtaining sufficient numbers of pre- and postchemotherapy human samples, we have not reached definite conclusion. However, analysis of seven paired specimens suggests the possibility that IGF signaling can modulate therapeutic sensitivity in human osteosarcoma. Activation of IGF signaling in regions that are separated from the vasculature might allow the survival of stressed tumor cells until resuming proliferation after "angiogenic switch" (38). Such "niches" or "hotbeds" of surviving tumor cells might thus engender minimal residual disease (Supplementary Fig. S6C).

The survival of osteosarcoma cells supported by IGF2 or insulin was found to be dependent on enhanced autophagy flux and glutamine availability. Both intra- and extracellular increased glutamine levels were suggested to be linked to upregulation of autophagy flux and protection from cell death (39, 40). Quiescent hematopoietic stem cells have also been suggested to be dependent on autophagy flux for their survival (41, 42). In addition, inhibition of metabolic processes or autophagy flux in quiescent fibroblasts or therapy-induced senescent lymphoma cells resulted in cell death (43, 44). Therefore, intracellular events underlying IGF2- or insulin-mediated dormancy in osteosarcoma cells might be common to quiescence induced in other cell types by other stimuli. Targeting of IGF- or insulin-mediated dormant cancer cells combined with conventional therapies might thus provide a firmer basis for the development of new options to overcome therapeutic resistance in individuals with osteosarcoma.

Disclosure of Potential Conflicts of Interest

T. Ishikawa is a researcher at Daiichi Sankyo Co. Ltd. H. Saya reports receiving commercial research grants from Daiichi-Sankyo Inc. and Eisai Co. Ltd. No potential conflicts of interest were disclosed by the other authors .

Authors' Contributions

Conception and design: T. Shimizu, A. Ueki, H. Saya
Development of methodology: T. Shimizu, T. Nagai
Acquisition of data (provided animals, acquired and managed patients, provided facilities, etc.): T. Shimizu, S. Tamaki, Y. Koyama, W. Kamel, T. Chiyoda, H. Ikeda, J. Kamei, K. Matsuo, J. Toguchida
Analysis and interpretation of data (e.g., statistical analysis, biostatistics, computational analysis): T. Shimizu, S. Tamaki, S. Osuka, H. Ikeda, J. Toguchida
Writing, review, and/or revision of the manuscript: T. Shimizu, H. Saya
Administrative, technical, or material support (i.e., reporting or organizing data, constructing databases): T. Shimizu, E. Sugihara, S. Yamaguchi-Iwai, T. Ishikawa, T. Chiyoda, S. Osuka, N. Onishi, Y. Fukuchi, A. Muto
Study supervision: T. Shimizu, Y. Toyama, A. Muto, H. Saya

Acknowledgments

The authors thank I. Ishimatsu for technical assistance as well as K. Arai and M. Sato for help with preparation of the article.

Grant Support

This work was supported by grants from the Ministry of Education, Culture, Sports, Science, and Technology of Japan (T. Shimizu and H. Saya), the Foundation for Promotion of Cancer Research of Japan (T. Shimizu), the Novartis Foundation for the Promotion of Science (T. Shimizu), and the National Institute of Biomedical Innovation of Japan (H. Saya).

The costs of publication of this article were defrayed in part by the payment of page charges. This article must therefore be hereby marked *advertisement* in accordance with 18 U.S.C. Section 1734 solely to indicate this fact.

Received April 1, 2014; revised September 16, 2014; accepted September 16, 2014; published OnlineFirst October 1, 2014.

References

1. Chou AJ, Geller DS, Gorlick R. Therapy for osteosarcoma: where do we go from here? Paediatr Drugs 2008;10:315–27.
2. Ritter J, Bielack SS. Osteosarcoma. Ann Oncol 2010;21 Suppl 7: vii320–5.
3. Jaffe N. Osteosarcoma: review of the past, impact on the future. The American experience. Cancer Treat Res 2009;152:239–62.
4. Redmond KM, Wilson TR, Johnston PG, Longley DB. Resistance mechanisms to cancer chemotherapy. Front Biosci 2008;13:5138–54.

Published OnlineFirst October 1, 2014; DOI: 10.1158/0008-5472.CAN-14-0914

5. Garraway LA, Janne PA. Circumventing cancer drug resistance in the era of personalized medicine. Cancer Discov 2012;2:214–26.
6. Glasspool RM, Teodoridis JM, Brown R. Epigenetics as a mechanism driving polygenic clinical drug resistance. Br J Cancer 2006; 94:1087–92.
7. Ivanov M, Kacevska M, Ingelman-Sundberg M. Epigenomics and interindividual differences in drug response. Clin Pharmacol Ther 2012;92:727–36.
8. Dylla SJ, Beviglia L, Park IK, Chartier C, Raval J, Ngan L, et al. Colorectal cancer stem cells are enriched in xenogeneic tumors following chemotherapy. PLoS One 2008;3:e2428.
9. Tehranchi R, Woll P, Anderson K, Buza-Vidas N, Mizukami T, Mead AJ. Persistent malignant stem cells in del(5q) myelodysplasia in remission. N Engl J Med 2010;363:1025–37.
10. Li X, Lewis MT, Huang J, Gutierrez C, Osborne K, Wu MF, et al. Intrinsic resistance of tumorigenic breast cancer cells to chemotherapy. J Natl Cancer Inst 2008;100:672–9.
11. Shimizu T, Ishikawa T, Sugihara E, Kuninaka S, Miyamoto T, Mabuchi Y, et al. c-MYC overexpression with loss of Ink4a/Arf transforms bone marrow stromal cells into osteosarcoma accompanied by loss of adipogenesis. Oncogene 2010;29:5687–99.
12. Shimizu T, Ishikawa T, Iwai S, Ueki A, Sugihara E, Onishi N, et al. Fibroblast growth factor-2 is an important factor that maintains cellular immaturity and contributes to aggressiveness of osteosarcoma. Mol Cancer Res 2012;10:454–68.
13. Chiyoda T, Sugiyama N, Shimizu T, Naoe H, Kobayashi Y, Ishizawa J, et al. LATS1/WARTS phosphorylates MYPT1 to counteract PLK1 and regulate mammalian mitotic progression. J Cell Biol 2012;197:625–41.
14. Ogawa Y, Yamazaki K, Kuwana M, Mashima Y, Nakamura Y, Ishiba S, et al. A significant role of stromal fibroblasts in rapidly progressive dry eye in patients with chronic GVHD. Invest Ophthalmol Vis Sci 2001;42:111–9.
15. Pollak M. The insulin and insulin-like growth factor receptor family in neoplasia: an update. Nat Rev Cancer 2012;12:159–69.
16. Valeriote F, van Putten L. Proliferation-dependent cytotoxicity of anticancer agents: a review. Cancer Res 1975;35:2619–30.
17. Rogakou EP, Pilch DR, Orr AH, Ivanova VS, Bonner WN. DNA double-stranded breaks induce histone H2AX phosphorylation on serine 139. J Biol Chem 1998;273:5858–68.
18. Rogakou EP, Boon C, Redon C, Bonner WN. Megabase chromatin domains involved in DNA double-strand breaks *in vivo*. J Cell Biol 1999;146:905–16.
19. Luo W, Kinsey M, Schiffman JD, Lessnick SL. Glutathione s-transferases in pediatric cancer. Front Oncol 2011;1;1–11.
20. Kabeya Y, Mizushima N, Ueno T, Yamamoto A, Kirisako T, Noda T, et al. LC3, a mammalian homologue of yeast Apg8p, is localized in autophagosome membranes after processing. EMBO J 2000;19: 5720–8.
21. Mizushima N, Komatsu M. Autophagy: renovation of cells and tissues. Cell 2011;147:728–41.
22. Yang ZJ, Chee CE, Huang S, Sinicrope FA. The role of autophagy in cancer: therapeutic implications. Mol Cancer Ther 2011;10:1533–41.
23. Tanida I, Mizushima N, Kiyooka M, Ohsumi M, Ueno T, Ohsumi Y, et al. Apg7p/Cvt2p: a novel protein-activating enzyme essential for autophagy. Mol Biol Cell 1999;10:1367–79.
24. Oettgen HF, Old LJ, Boyse EA, Campbell HA, Philips FS, Clarkson BD, et al. Inhibition of leukemia in man by L-asparaginase. Cancer Res 1967;27:2619–31.
25. Arai F, Hirao A, Ohmura M, Sato H, Matsuoka S, Takubo K, et al. Tie2/Angiopoietin-1 signaling regulates hematopoietic stem cell quiescence in the bone marrow niche. Cell 2004;118:149–61.
26. Ema H, Suda T. Two anatomically distinct niches regulate stem cell activity. Blood 2012;120:2174–81.
27. Adam AP, George A, Schewe D, Bragado P, Iglesias BV, Ranganathan AC, et al. Computational identification of a p38SAPK-regulated transcription factor network required for tumor cell quiescence. Cancer Res 2009;69:5664–72.
28. Sosa MS, Avivar-Valderas A, Bragado P, Wen HC, Aguirre-Ghiso JA. Erk1/2 and p38α/β signaling in tumor cell quiescence: opportunities to control dormant residual disease. Clin Cancer Res 2011;17:5850–7.
29. Chandarlapaty S. Negative feedback and adaptive resistance to the targeted therapy of cancer. Cancer Discov 2012;2:311–9.
30. Haruta T, Uno T, Kawahara J, Takano A, Egawa K, Sharma PM, et al. A rapamycin-sensitive pathway down-regulates insulin signaling via phosphorylation and proteasomal degradation of insulin receptor substrate-1. Mol Endocrinol 2000;14:783–94.
31. Tremblay F, Brule S, Um SH, Li Y, Masuda K, Roden M, et al. Identification of IRS-1 Ser-1101 as a target of S6K1 in nutrient- and obesity-induced insulin resistance. Proc Natl Acad Sci USA 2007; 104:14056–61.
32. Tanti JF, Jager J. Cellular mechanisms of insulin resistance: role of stress-regulated serine kinases and insulin receptor substrates (IRS) serine phosphorylation. Curr Opin Pharmacol 2009;9:753–62.
33. Li B, Tsao SW, Chan KW, Ludwig DL, Novosyadlyy R, Li YY, et al. Id1-induced IGF-II and its autocrine/endocrine promotion of esophageal cancer progression and chemoresistance - Implications for IGF-II and IGF-1R-targeted therapy. Clin Cancer Res 2014;20:2651–62.
34. Avnet S, Sciacca L, Salerno M, Gancitano G, Cassarino MF, Longhi A, et al. Insulin receptor isoform A and insulin-like growth factor II as additional treatment targets in human osteosarcoma. Cancer Res 2009;69:2443–52.
35. Pollak MN, Polychronakos C, Richard M. Insulin like growth factor I: a potent mitogen for human osteogenic sarcoma. J Natl Cancer Inst 1990;82:301–5.
36. Pollak M, Sem AW, Richard M, Tetenes E, Bell R. Inhibition of metastatic behavior of murine osteosarcoma by hypophysectomy. J Natl Cancer Inst 1992;84:966–71.
37. MacEwen EG, Pastor J, Kutzke J, Tsan R, Kurzman ID, Thamm DH, et al. IGF-1 receptor contributes to the malignant phenotype in human and canine osteosarcoma. J Cell Biochem 2004;92:77–91.
38. Ribatti D, Nico B, Crivellato E, Roccaro AM, Vacca A. The history of the angiogenic switch concept. Leukemia 2007;21:44–52.
39. van der Vos KE, Eliasson P, Cezanne TP, Vervoort SJ, van Boxtel R, Putker M, et al. Modulation of glutamine metabolism by the PI(3)K-PKB-FOXO network regulates autophagy. Nature Cell Biol 2012;14: 829–37.
40. Sakiyama T, Musch MW, Ropeleski MJ, Tsubouchi H, Chang EB. Glutamine increases autophagy under basal and stressed conditions in intestinal epithelial cells. Gasteroenterology 2009;136:924–32.
41. Warr MR, Binnewies M, Flach J, Reynaud D, Garg T, Malhotra R, et al. FOXO3A directs a protective autophagy program in haematopoietic stem cells. Nature 2013;494:323–9.
42. Mortensen M, Soilleux EJ, Djordjevic G, Tripp R, Lutteropp M, Sadighi-Akha E, et al. The autophagy protein Atg7 is essential for hematopoietic stem cell maintenance. J Exp Med 2011;208:455–67.
43. Lemons JMS, Feng XJ, Bennett BD, Legesse-Miller A, Johnson EL, Raitman I, et al. Quiescent fibroblasts exhibit high metabolic activity. PLoS Biol 2010;8:e1000514.
44. Dorr JR, Yu Y, Milanovic M, Beuster G, Zasada C, Dabritz HM, et al. Synthetic lethal metabolic targeting of cellular senescence in cancer therapy. Nature 2013;501:421–5.

Published OnlineFirst October 1, 2014; DOI: 10.1158/0008-5472.CAN-14-0914

Cancer Research

IGF2 Preserves Osteosarcoma Cell Survival by Creating an Autophagic State of Dormancy That Protects Cells against Chemotherapeutic Stress

Takatsune Shimizu, Eiji Sugihara, Sayaka Yamaguchi-Iwai, et al.

Cancer Res 2014;74:6531-6541. Published OnlineFirst October 1, 2014.

GENETIC TESTING AND MOLECULAR BIOMARKERS
Volume 18, Number 11, 2014

Pp. 722–735
DOI: 10.1089/gtmb.2014.0109

The Use of Next-Generation Sequencing in Molecular Diagnosis of Neurofibromatosis Type 1: A Validation Study

Ryo Maruoka,[1,2] Toshiki Takenouchi,[1,3] Chiharu Torii,[1] Atsushi Shimizu,[4] Kumiko Misu,[1] Koichiro Higasa,[5] Fumihiko Matsuda,[5] Arihito Ota,[6] Katsumi Tanito,[6] Akira Kuramochi,[7] Yoshimi Arima,[8] Fujio Otsuka,[9] Yuichi Yoshida,[10] Keiji Moriyama,[2] Michihito Niimura,[6] Hideyuki Saya,[8] and Kenjiro Kosaki[1]

Aims: We assessed the validity of a next-generation sequencing protocol using in-solution hybridization-based enrichment to identify *NF1* mutations for the diagnosis of 86 patients with a prototypic genetic syndrome, neurofibromatosis type 1. In addition, other causative genes for classic genetic syndromes were set as the target genes for coverage analysis. *Results:* The protocol identified 30 nonsense, 19 frameshift, and 8 splice-site mutations, together with 10 nucleotide substitutions that were previously reported to be pathogenic. In the remaining 19 samples, 10 had single-exon or multiple-exon deletions detected by a multiplex ligation-dependent probe amplification method and 3 had missense mutations that were not observed in the normal Japanese SNP database and were predicted to be pathogenic. Coverage analysis of the genes other than the *NF1* gene included on the same diagnostic panel indicated that the mean coverage was 115-fold, a sufficient depth for mutation detection. *Conclusions:* The overall mutation detection rate using the currently reported method in 86 patients who met the clinical diagnostic criteria was 92.1% (70/76) when 10 patients with large deletions were excluded. The results validate the clinical utility of this next-generation sequencing-based method for the diagnosis of neurofibromatosis type 1. Comparable detection rates can be expected for other genetic syndromes, based on the results of the coverage analysis.

Introduction

GENETIC TESTING HAS HELPED clinicians to define the molecular pathology of diseases, especially when patients present with an atypical combination of phenotypic features. Our group developed a custom-designed mutation analysis panel using denaturing high-pressure liquid chromatography for the systematic screening of patients with classic genetic syndromes (Kosaki *et al.*, 2005). The system can be used to screen all the exons of the candidate gene quickly and has been helpful in confirming the clinical diagnosis, as published in a series of reports in this journal (Udaka *et al.*, 2005, 2006, 2007; Aramaki *et al.*, 2006; Samejima *et al.*, 2007; Hattori *et al.*, 2009). Nevertheless, the throughput of the system was not high enough to screen multiple candidate genes in a single testing.

The recent advent of a target sequencing panel with the next-generation sequencing technology has enabled many genes, regardless of size, to be analyzed in a systematic and comprehensive manner, as reviewed in this journal (Yan *et al.*, 2013). The strength of such a comprehensive approach is the ability to detect atypical presentations of classic syndromes, as illustrated by our recent reports on several patients with atypical presentations of mutations in the causative

[1]Center for Medical Genetics, Keio University School of Medicine, Tokyo, Japan.
[2]Section of Maxillofacial Orthognathics, Division of Maxillofacial/Neck Reconstruction, Department of Maxillofacial Reconstruction and Function, Graduate School, Tokyo Medical and Dental University, Tokyo, Japan.
[3]Department of Pediatrics, Keio University School of Medicine, Tokyo, Japan.
[4]Division of Biomedical Information Analysis, Iwate Tohoku Medical Megabank Organization, Iwate Medical University, Iwate, Japan.
[5]Center for Genomic Medicine, Kyoto University Graduate School of Medicine, Kyoto, Japan.
[6]Department of Dermatology, Jikei University School of Medicine, Tokyo, Japan.
[7]Department of Dermatology, Saitama Medical University, Saitama, Japan.
[8]Division of Gene Regulation, Institute for Advanced Medical Research, Keio University School of Medicine, Tokyo, Japan.
[9]Department of Dermatology, Institute of Clinical Medicine, University of Tsukuba, Tsukuba, Japan.
[10]Division of Dermatology, Department of Medicine of Sensory and Motor Organs, Faculty of Medicine, Tottori University, Yonago, Japan.

genes of three classic genetic syndromes: the neonatal progeroid presentation of an *FBN1* mutation (Takenouchi *et al.*, 2013a), the Noonan-cafe au lait syndrome-like presentation of a *MAP2K2* mutation (Takenouchi *et al.*, 2013b), and Stickler syndrome-like presentation of *SOX9* mutation (Takenouchi *et al.*, 2014).

In this study, we assessed the analytical and clinical validity of the next-generation sequencing protocol with in-solution hybridization-based enrichment to identify disease-causing mutations in the diagnosis of a prototypic genetic syndrome, neurofibromatosis type 1, compared with direct capillary sequencing, which is the current gold standard methodology. The reason for the choice of the *NF1* gene, the causative gene for neurofibromatosis type 1, was twofold: (1) neurofibromatosis type 1 is a relatively common genetic condition with readily recognizable phenotypes: café-au-lait spots, cutaneous neurofibromas, axillary and inguinal freckling, and Lisch nodules (iris hamartomas) (Carey and Viskochil, 1999) and (2) the *NF1* gene comprised a total of 58 exons and is one of the largest genes in the human genome, making it a relatively difficult clinical target for direct capillary sequencing.

Materials and Methods

Patients

The current research protocol was approved by the institutional review board of Keio University and each participating center. Eighty-six patients with neurofibromatosis type 1 who met the NIH clinical diagnostic criteria (Neurofibromatosis Conference Statement, 1988) were recruited from multiple centers participating in the project. The NIH diagnostic criteria for neurofibromatosis type 1 defines an individual as neurofibromatosis type 1 when the person has two or more of the following features: six or more café-au-lait macules with a maximum diameter of over 5 mm in prepubertal individuals and with a maximum diameter of over 15 mm in postpubertal individuals; two or more neurofibromas of any type or 1 plexiform neurofibroma; freckling in the axillary or inguinal regions; optic glioma, two or more Lisch nodules; a distinctive osseous lesion, such as sphenoid dysplasia or tibial pseudarthrosis; and a first-degree relative (parent, sibling, or offspring) with neurofibromatosis type 1, as defined according to the above-mentioned criteria. After written consent was obtained at each participating center, the whole blood samples were sent to Keio University for genetic analysis.

Genomic DNA, sample preparation, targeted capturing, sequencing

Genomic DNA was extracted from peripheral blood according to standard procedures using the phenol–chloroform extraction method and checked for quality using Qubit (Life Technologies). The genomic DNA (3 μg) was fragmented into ~150 bp. In-solution hybridization-based enrichment was performed using the SureSelect Target Enrichment system (Agilent Technologies). The *NF1* gene (the canonical Refseq transcript NM_001042492.2) together with 108 causative genes for the more common classical congenital malformation syndromes selected from a standard textbook (Jones, 2005) was set as the target gene (Table 1). Genes that are responsible for a disease phenotype and involved in the RAS pathway (i.e., Rasopathy genes) (Aoki *et al.*, 2008) were included in the 108 genes set. A biotinylated RNA capture library was designed using the eArray system (Agilent Technologies) according to the manufacturer's protocol. The captured DNA was subjected to a 150-bp paired-end read sequencing on the MiSeq system (Illumina).

Bioinformatics pipeline

The sequence reads from the sequencer were exported as FASTQ format files and were analyzed using sets of open-source programs by means of the default parameters; the sequence reads were aligned to the human reference genome DNA sequence (hs37d5 assembly) using the Burrows–Wheeler Alignment (BWA) tool version 0.6.1 (Li and Durbin, 2009). The Genome Analysis Toolkit (GATK) package (McKenna *et al.*, 2010) was used to perform local realignment, base quality score recalibration, and SNP/indel calls. The called SNPs/indels were annotated using snpEff version 3.1 (Cingolani *et al.*, 2012), regarded as nonpathogenic, and excluded from further analysis when they were observed in the 1000 Genomes Project (www.1000genomes.org/) or in the Japanese SNP dataset of 1208 normal individuals (Japanese Genetic Variation Consortium, 2013). The variants and alignments were visually inspected using the Integrative Genomics Viewer version 2.1 (Thorvaldsdóttir *et al.*, 2013) and VarSifter version 1.5 (Teer *et al.*, 2012). Variants in the RAS pathway, including *PTPN11*, *KRAS*, *SOS1*, *RAF1*, *SHOC2*, *HRAS*, *BRAF*, *MAPK1*, *MAP2K1*, *MAP2K2*, *MAPK3*, *SPRED1*, and *RASA1*, were evaluated for pathogenicity. Other genes were not subject to further variant analysis to avoid potential issues with incidental findings. A statistical coverage analysis was performed as described below.

Coverage analysis

Information about enrichment performance and target coverage was obtained using the software NGSrich version 0.7.8 (Frommolt *et al.*, 2012). The following parameters were measured: information about the number of reads, mean coverage, fraction of the target region with a particular depth across the 109 genes, information on the number of genes that are poorly covered, and a summary table with exon-specific coverage information at the *NF1* locus.

Direct capillary sequencing for validation

When the next-generation sequencing protocol identified truncating mutations, including nonsense mutations, frameshift mutations, and mutations at the canonical splice sites, or missense mutations that had been previously reported as being pathogenic in the literature, the variants were validated with direct capillary sequencing. In the remaining samples, all the exons were analyzed using direct capillary sequencing (Richards *et al.*, 2008). For direct capillary sequencing, 56 pairs of polymerase chain reaction (PCR) primers were designed on flanking intronic and untranslated regions to encompass the coding regions of the 58 *NF1* exons and at least 30 bp of the intronic sequence surrounding each exon (Table 2). Three primers were designed newly using primer design software, Primer3 (Rozen and Skaletsky, 2000), and the remaining primers were described elsewhere (Purandare *et al.*,

TABLE 1. LIST OF THE 109 GENES

Gene	*Chromosome*	*Basepair position (GRCh37)*	*Disease*	*Gene*	*Chromosome*	*Basepair position (GRCh37)*	*Disease*
ACTA2	10	90,694,830–90,751,146	Multisystemic smooth muscle dysfunction syndrome	*MSX1*	4	4,861,391–4,865,662	Witkop syndrome
ACTC1	15	35,080,296–35,087,926	Atrial septal defect	*MYH7*	14	23,881,946–23,904,869	Scapuloperoneal syndrome, myopathic type
ACVRL1	12	52,300,656–52,317,144	Hereditary hemorrhagic telangiectasia	*MYH9*	22	36,677,322–36,784,106	Fechtner syndrome
BRAF	7	140,415,748–140,624,563	Cardiofaciocutaneous syndrome	*NF1*	17	29,421,944–29,704,694	Neurofibromatosis type 1
CBL	11	119,076,985–119,178,858	Noonan syndrome-like disorder	*NIPBL*	5	36,876,860–37,065,925	Cornelia de Lange syndrome
CDKL5	X	18,443,724–18,671,748	Angelman syndrome-like disorder	*NOTCH2*	1	120,454,175–120,639,879	Alagille syndrome
CHD7	8	61,591,320–61,780,586	CHARGE syndrome	*NRAS*	1	115,247,084–115,259,514	Noonan syndrome
COL11A1	1	103,342,022–103,574,051	Fibrochondrogenesis	*NRTN*	19	5,823,817–5,828,334	Hirschsprung disease
COL11A2	6	33,130,468–33,160,244	Stickler syndrome	*NSD1*	5	176,560,025–176,727,213	Sotos syndrome
COL1A1	17	48,261,456–48,279,002	Osteogenesis imperfecta	*OTX2*	14	57,267,424–57,277,193	Syndromic microphthalmia
COL1A2	7	94,023,872–94,060,543	Ehlers-Danlos syndrome	*PHOX2B*	4	41,746,098–41,750,986	Congenital central hypoventilation syndrome
COL2A1	12	48,366,747–48,398,284	Stickler syndrome	*PKHD1*	6	51,480,144–51,952,422	Polycystic kidney and hepatic disease
COL3A1	2	189,839,098–189,877,471	Ehlers-Danlos syndrome	*PLOD1*	1	11,994,723–12,035,598	Ehlers-Danlos syndrome
COL5A1	9	137,533,650–137,736,688	Ehlers-Danlos syndrome	*PSPN*	19	6,375,304–6,375,859	Hirschsprung's disease
COL5A2	2	189,896,640–190,044,667	Ehlers-Danlos syndrome	*PTCH1*	9	98,205,263–98,279,246	Basal cell nevus syndrome
COL9A1	6	70,925,742–71,012,785	Stickler syndrome	*PTPN11*	12	112,856,535–112,947,716	LEOPARD syndrome
COL9A2	1	40,766,161–40,782,938	Stickler syndrome	*RAD21*	8	117,858,172–117,887,104	Cornelia de Lange syndrome
COMP	19	18,893,582–18,902,113	Epiphyseal dysplasia	*RAF1*	3	12,625,099–12,705,699	LEOPARD syndrome
CREBBP	16	3,775,054–3,930,120	Rubinstein-Taybi syndrome	*RASA1*	5	86,564,069–86,687,742	Parkes Weber syndrome
CUL7	6	43,005,354–43,021,682	3-M syndrome	*RET*	10	43,572,516–43,625,798	MENII
DCC	18	49,866,541–51,062,272	Mirror movements	*RUNX2*	6	45,296,053–45,518,818	Cleidocranial dysplasia
DDX3X	X	41,192,560–41,209,526	Medulloblastoma	*SALL1*	16	51,169,885–51,185,182	Townes–Brocks syndrome
ECE1	1	21,543,739–21,672,033	Hirschsprung disease	*SALL4*	20	50,400,550–50,419,058	Duane-radial ray syndrome
EDN3	20	57,875,498–57,901,046	Central hypoventilation syndrome	*SCN1B*	19	35,521,554–35,531,352	Brugada syndrome
EDNRB	13	78,469,615–78,549,663	Waardenburg syndrome	*SHH*	7	155,595,557–155,604,966	Holoprosencephaly
EFNB1	X	68,048,839–68,062,006	Craniofrontonasal dysplasia	*SHOC2*	10	112,679,300–112,773,424	Noonan-like syndrome
ENG	9	130,577,290–130,617,051	Heredity hemorrhagic telangiectasia	*SIX3*	2	45,169,036–45,173,215	Holoprosencephaly

(*continued*)

TABLE 1. (CONTINUED)

Gene	Chromosome	Basepair position (GRCh37)	Disease	Gene	Chromosome	Basepair position (GRCh37)	Disease
EP300	22	41,488,613–41,576,080	Rubinstein-Taybi syndrome	*SIX6*	14	60,975,937–60,978,524	Microphthalmia with cataract
FBN1	15	48,700,502–48,937,984	Acromicric dysplasia	*SMC1A*	X	53,401,069–53,449,676	Cornelia de Lange syndrome
FBN2	5	127,593,600–127,873,734	Congenital contractural arachnodactyly	*SMC3*	10	112,327,448–112,364,391	Cornelia de Lange syndrome
FGFR1	8	38,268,655–38,326,351	Hypogonadotropic hypogonadism	*SOS1*	2	39,208,689–39,347,685	Noonan syndrome
FGFR2	10	123,237,843–123,357,971	Antley-Bixler syndrome	*SOX10*	22	38,368,318–38,380,555	PCWH syndrome
FGFR3	4	1,795,038–1,810,598	Achondroplasia	*SOX2*	3	181,429,711–181,432,223	Syndromic microphthalmia
GDNF	5	37,812,778–37,839,781	Central hypoventilation syndrome	*SPRED1*	15	38,544,924–38,649,449	Legius syndrome
GFRA1	10	117,816,435–118,033,125	Hirschsprung's disease	*SPRY2*	13	80,910,110–80,915,085	Holoprosencephaly
GFRA2	8	21,549,529–21,672,391	Hirschsprung's disease	*STAG1*	3	136,055,077–136,471,220	Cornelia de Lange syndrome
GLA	X	100,652,778–100,663,000	Fabry disease	*TAZ*	X	153,639,876–153,650,064	Barth syndrome
HRAS	11	532,241–535,560	Costello syndrome	*TBX22*	X	79,270,254–79,287,267	Abruzzo-Erickson syndrome
IHH	2	219,919,141–219,925,237	Acrocapitofemoral dysplasia	*TBX5*	12	114,791,734–114,846,246	Holt-Oram syndrome
IRF6	1	209,958,967–209,979,519	Van der Woude syndrome	*TCF4*	18	52,889,561–53,303,251	Pitt-Hopkins syndrome
JAG1	20	10,618,331–10,654,693	Alagille syndrome	*TCOF1*	5	149,737,201–149,779,870	Treacher Collins syndrome
KCNE1	21	35,790,909–35,884,572	Jervell and Lange-Nielsen syndrome	*TGFBR1*	9	101,867,411–101,916,473	Loeys-Dietz syndrome
KCNJ2	17	68,164,756–68,176,188	Andersen syndrome	*TGFBR2*	3	30,647,993–30,735,633	Loeys-Dietz syndrome
KCNQ1	11	2,466,220–2,870,339	Jervell and Lange-Nielsen syndrome	*TGIF1*	18	3,411,924–3,458,408	Holoprosencephaly
KIAA1279	10	70,748,476–70,776,738	Goldberg-Shprintzen megacolon syndrome	*TP63*	3	189,348,941–189,615,067	EEC syndrome
KIF26A	14	104,605,059–104,647,234	Megacolon	*TRAPPC10*	21	45,432,205–45,526,432	Holoprosencephaly
KRAS	12	25,358,179–25,403,869	Noonan syndrome	*TRIM37*	17	57,059,998–57,184,265	Mulibrey nanism
L1CAM	X	153,126,968–153,151,627	CRASH syndrome	*TSC1*	9	135,766,734–135,820,093	Tuberous sclerosis
LAMP2	X	119,560,002–119,603,203	Danon disease	*TSC2*	16	2,097,471–2,138,712	Tuberous sclerosis
MAP2K1	15	66,679,181–66,783,881	Cardiofaciocutaneous syndrome	*TWIST1*	7	19,039,314–19,157,294	Saethre Chotzen syndrome
MAP2K2	19	4,090,318–4,124,125	Cardiofaciocutaneous syndrome	*VHL*	3	10,183,318–10,195,353	Von Hippel-Lindau syndrome
MAPK1	22	22,113,945–22,221,969	Acromesomelic dysplasia	*VSX2*	14	74,706,174–74,729,440	Microphthalmia
MAPK3	16	30,125,425–30,134,629	Cardiac hypertrophy	*ZEB2*	2	145,141,941–145,277,957	Mowat-Wilson syndrome
MECP2	X	153,287,024–153,363,187	Rett syndrome	*ZIC2*	13	100,634,025–100,639,018	Holoprosencephaly
MID1	X	10,413,349–10,851,828	Opitz GBBB syndrome				

Table 2. List of Polymerase Chain Reaction Primers

Exon	*Primer sequence (5′-3′)*	*Amplicon size*	*Reference*	*Exon*	*Primer sequence (5′-3′)*	*Amplicon size*	*Reference*
1	CAGACCCTCTCCTTGCCTCTT GGATGGAGGGTCGGAGGCTG	439	Purandare *et al.* (1995)	29	ATATGGAGCAGGTATAATAAAC AAAACAGCGGTTCTATGTG	181	Bausch *et al.* (2007)
2	CGTCATGATTTTCAATGGCAAG GCTCACTGAATCTAAAACCCAGC	438	Bausch *et al.* (2007)	30	CGTTGCACTTGGCTTAATGTCTG CCATCAGCAGCTAGATCCTTCTTT	327	Bausch *et al.* (2007)
3	TTTCACTTTTCAGATGTGTGTTG TGGTCCACATCTGTACTTTG	245	Purandare *et al.* (1995)	31	TTTTCTGTGATTCATAGCC GATATTCTTAACAAACAGCA	400	This report
4	TTAAATCTAGGTGGTGTGT AAACTCATTTCTCTGGAG	517	Han *et al.* (2001)	32	CTTATACTCAATTCTCAACTCC GAATTTAAGATAGCTAGATTATC	226	Bausch *et al.* (2007)
5	GAGATACCACACCTGTCCCCTAA TTGACCCAGTGATTTTTTTCAGA	215	Bausch *et al.* (2007)	33	GACTTCATACAATAAATAATCTG TATTTGATTCAAACAGAGCAAC	195	Bausch *et al.* (2007)
6	TTTCCTAGCAGACAACTATCGA AGGATGCTAACAACAGCAAAT	308	Han *et al.* (2001)	34	CTCCATATTTGTAATCTTAGTTA GGAGAGTGTTCACTATCCC	298	Bausch *et al.* (2007)
7	GAAGGAAGTTAGAAGTTTGTG CACAAGTAGGCATTTAAAAGA	211	Bausch *et al.* (2007)	35	GTTACAAGTTAAAGAAATGTGTAG CTAACAAGTGGCCTGGTGGCAAAC	298	Purandare *et al.* (1995)
8	CATGTTTATCTTTTAAAAATGTTGCC ATAATGGAAATAATTTTGCCCTCC	301	Han *et al.* (2001)	36	TTTATTGTTTATCCAATTATAGACTT TCCTGTTAAGTCAACTGGGAAAAAC	296	Purandare *et al.* (1995)
9	CTGTTAATTTGCTATAATATTAGC CATAATACTTATGCTAGAAAATTC	328	Bausch *et al.* (2007)	37	TGAATCCAGACTTTGAAGAATTGTT CTAGGGAGGCCAGGATATAGTCTAGT	644	Bausch *et al.* (2007)
10	GTAATGTGTTGATGTTATTACATG GTCTTTTTGTTTATAAAGGATAACA	273	Bausch *et al.* (2007)	38	GGTTGGTTTCTGGAGCCTTTTAGA CAACAAACCCCAAATCAAACTGA	467	Bausch *et al.* (2007)
11	CTTTCTATTTGCTGTTCTTTTTGG CCTTTTTGAAAACCAAGAGTGCA	264	Bausch *et al.* (2007)	39	TTGGAACTATAAGGAAAAATACGTTT AGGGTTTTCTTTGAATTCTCTTAGA	321	Bausch *et al.* (2007)
12	ACGTAATTTTGTACTTTTTCTTCC CAATAGAAAGGAGGTGAGATTC	222	Purandare *et al.* (1995)	40	ATAATTGTTGATGTGATTTTCATTG AATTTTGAACCAGATGAAGAG	424	Han *et al.* (2001)
13	GCAAAAACGATTTTCATTGTTTTGT GCGTTTCAGCTAAACCCAATT	403	This report	41	TTGATTAGGCTGTTCCAATGAA CAAAACAAAAAACCTCCTGATGAT	298	Bausch *et al.* (2007)
14	ATTGAAGTTTCCTTTTTTTCCTTG GTATAGACATAAACATACCATTTC	275	Bausch *et al.* (2007)	42	GTGCTAAAACTTTGAGTCCCATGT ATAATCTATATTGATCAGGTGAAGTA	415	Bausch *et al.* (2007)
15	CCAAAAATGTTTGAGTGAGTCT ACCATAAAACCTTTGGAAGTG	256	Han *et al.* (2001)	43	GCAAGGAGCATTAATACAATGTATC CCATGCAAGTGTTTTTATTTAAGC	507	Bausch *et al.* (2007)

(*continued*)

TABLE 2. (CONTINUED)

Exon	*Primer sequence (5′-3′)*	*Amplicon size*	*Reference*	*Exon*	*Primer sequence (5′-3′)*	*Amplicon size*	*Reference*
16	AAACCTTACAAGAAAAACTAAGCT ATTACCATTCCAAATATTCTTCCA	303	Purandare *et al.* (1995)	44–45	GGTAACAGGTCACTTAATGACATCA GACCTCAAATTTAAACGTCTTTTAGA	512	Bausch *et al.* (2007)
17	CTCTTGGTTGTCAGTGCTTC CAGAAAACAAACAGAGCACAT	261	Han *et al.* (2001)	46	CATTCCGAGATTCAGTTTAGGAG AAGTAACATTCAACACTGATACCC	236	Abernathy *et al.* (1997)
18	CCCAAGTTGCAAATATATGTC GTGCTTTGAGGCAGACTGAG	336	Bausch *et al.* (2007)	47	TCCCCAAAAGAGAAAACATGG AGCAACAAGAAAAGATGGAAGAGT	334	Bausch *et al.* (2007)
19	TGAAGCATTTGCTCTGCTCT GTTTCAAACTTGATGTATATTAAA	347	Bausch *et al.* (2007)	48	CTACTGTGTGAACCTCATCAACC GTAAGACATAAGGGCTAACTTACTTC	284	Abernathy *et al.* (1997)
20	ACTTGGCTGTAGCTGATTGA ACTTTACTGAGCGACTCTTGAA	247	Han *et al.* (2001)	49	TCAGGGAAGAAGACCTCAGCAGATGC TGAACTTTCTGCTCTGCCACGCAACC	328	Abernathy *et al.* (1997)
21	GGAAGAAATGTTGGATAAAGCA AAACAAGTCACTCTATTCATAGA	579	Bausch *et al.* (2007)	50	GTGCACATTTAACAGGTACTAT CTTCCTAGGCCATCTCTAGAT	373	Han *et al.* (2001)
22	TATCTGTATGCTTATTTGGCTCTA GTGCAGTAAAGAATGGCCAG	385	Bausch *et al.* (2007)	51	CTTGGAAGGAGCAAACGATGGTTG CAAAAACTTTGCTACACTGACATGG	356	Abernathy *et al.* (1997)
23	AGAAGTTGTGTACGTTCTTTTCT CTCCTTTCTACCAATAACCGC	367	Purandare *et al.* (1995)	52	GCTCCAGGGATGTATTAGAGCTTT TGACTTTCATGTACTCTCCCACCT	325	Bausch *et al.* (2007)
24	TTGTTCCCTTCTGGCTTTTAT ATCTCAAAAGTTTAAATACACA	365	This report	53–54	TGAAGTGATTATCCAGGTGTTTGA AAAGACAGGCACGAAGGTGA	506	Bausch *et al.* (2007)
25	TGAGGGGAAGTGAAAGAACT GGCTTTATTTGCTTTTTGCT	235	Han *et al.* (2001)	55	AATTTTGGCACATTATTCTGGG AGCAAGTTCATCAACCATCCTT	290	Bausch *et al.* (2007)
26	CCACCCTGGCTGATTATCG TAATTTTTGCTTCTCTTACATGC	402	Purandare *et al.* (1995)	56	CTGTTACAATTAAAAGATACCTTGC TGTGTGTTCTTAAAGCAGGCATAC	185	Abernathy *et al.* (1997)
27	TGGTCTCATGCACTCCATA CATCTTTCTTCTGGCTCTGA	474	Han *et al.* (2001)	57	TTTTGGCTTCAGATGGGGATTTAC AAGGGAATTCCTAATGTTGGTGTC	351	Abernathy *et al.* (1997)
28	TGCTACTCTTTAGCTTCCTAC CCTTAAAAGAAGACAATCAGCC	331	Purandare *et al.* (1995)	58	AAGCGACACATGACTGCAATG TGGCTTTCATCACTGGCCA	571	Bausch *et al.* (2007)

1995; Abernathy *et al.*, 1997; Han *et al.*, 2001; Bausch *et al.*, 2007). The 3′ end of the primers were designed so as not to match the genomic sequences of any of the highly homologous pseudogene sequences to avoid mispriming to the pseudogenes. Direct capillary sequencing was performed using the ABI BigDye version 1.1 Terminator Cycle Kit (Life Technologies) and the ABI Prism 3500 Capillary Array Sequencer (Life Technologies). The sequence data were analyzed using Mutation Surveyor version 4.0.6 (Softgenetics) and Sequencher version 5.0 (Gene Codes Corp.).

Multiplex ligation-dependent probe amplification

When the next-generation sequencing protocol did not identify truncating mutations, canonical splice-site mutations, or other point mutations previously reported as pathological missense change or splicing defect, the remaining samples were screened for single/multiple exon deletions or duplications using a multiplex ligation-dependent probe amplification method (De Luca *et al.*, 2007) (SALSA P081/082-B2 NF1 MLPA assay kit; MRC-Holland) concurrently with the direct capillary sequencing of all the exons, as stated above.

Analysis algorithm of the variants

Missense variants that have not been reported as pathogenic in the literature and were not observed in the 1208 normal Japanese exome data were evaluated for potential pathogenicity using five bioinformatics programs, including SIFT (Kumar *et al.*, 2009), Polyphen2 (Adzhubei *et al.*, 2010), LRT (Chun and Fay, 2009), MutationTaster (Schwarz *et al.*, 2010), and PhyloP (Siepel *et al.*, 2009). When four of the five programs predicted the results as pathogenic ("damaging" with SIFT, "probably damaging" with PolyPhen2, "deleterious" with LRT, "disease causing" with MutationTaster, or "conserved" with PhyloP), we interpreted the clinical significance of the missense mutation as being putatively pathogenic.

Results

Performance of sequence capturing

In the custom-designed mutation analysis panel for the screening of classic genetic syndromes, the number of bases for targeted capturing was 459,952 bp over 1888 regions of the 109 target genes, including *NF1*. An average of 207,203 reads per sample were mapped and aligned uniquely to the targeted bases of the 109 genes among the 86 samples.

As far as the *NF1* locus was concerned, all the exons were highly covered with a coverage of 190.7x per sample. Overall, 99.3% of the regions were covered at least with a coverage of 5x and 98.8% of the regions were covered at least with a coverage of 30x. The mean coverage of all the exons in the 86 samples indicated that all the exons, but exon 1, were appropriate for base calling by next-generation sequencing (Table 3). Because of the poor coverage, exon 1 was sequenced using the direct capillary sequencing in all 86 samples, none of which had any variants.

The mean coverage over the entire targeted regions per sample was 131.0x, and most of the regions were well covered (Table 4). Overall, 97.1% of the regions were covered at least 5x coverage, and 84.4% of the regions were covered at least 30x coverage. Some exons of *NF1* and other regions were less well covered than others. Exon 15 and exon 50 of *NF1*, together with the *COMP* gene and the *PHOX2B* gene, had relatively low coverages of 86.9x, 79.1x, 55.3x, and 19.2x, respectively.

TABLE 3. MEAN COVERAGE OF *NF1* EXONS AMONG 86 PATIENTS

Exon	*Coverage (x)*	*Exon*	*Coverage (x)*
1	1.7	30	239.7
2	220.2	31	175.9
3	168.8	32	157.0
4	169.5	33	124.6
5	145.0	34	216.0
6	170.9	35	152.1
7	164.8	36	189.3
8	144.0	37	284.7
9	182.7	38	261.5
10	174.1	39	230.9
11	179.2	40	217.3
12	194.9	41	206.8
13	120.0	42	276.9
14	141.2	43	195.7
15	86.9	44	181.1
16	152.7	45	166.3
17	212.6	46	156.4
18	251.3	47	185.7
19	127.1	48	159.4
20	215.4	49	241.5
21	175.2	50	79.1
22	191.4	51	174.3
23	103.1	52	238.4
24	194.0	53	235.9
25	96.6	54	217.5
26	212.1	55	136.8
27	209.6	56	320.0
28	238.7	57	220.5
29	208.5	58	122.6

NF1 has seven highly homologous pseudogene sequences located in chromosomes other than chromosome 17 (2q12-q13, 12q11, 14p11-q11, 15q11.2, 18p11.2, 21p11-q11, and 22p11-q11), on which *NF1* resides (Upaddhyaya, 2008). We scrutinized the mapped reads among 10 arbitrarily selected patients; all the pseudogene sequences were mapped to their orthologous locations in the genome rather than the *NF1* locus on chromosome 17.

Coverage of the 108 genes other than the *NF1* gene was evaluated in all 86 samples. The mean coverage of all 108 genes on the same diagnostic panel indicated that the mean coverage ranged from 19.2x to 254.1x, with mean of 114.5x (Table 4).

Mutation detection

The next-generation sequencing protocol described above led to the identification of pathological *NF1* mutations in 70 of the 86 patients who met the NIH diagnostic criteria. The clinical information is listed in Table 5. All the 70 patients harbored mutations in a heterozygous state: 30 nonsense mutations, 19 frameshift mutations, 8 canonical splice-site mutations, and 6 point mutations that were previously reported and have been shown to lead to aberrant splicing

TABLE 4. SUMMARY OF THE COVERAGE OF 109 GENES

Gene	*Coverage (x)*	*Gene*	*Coverage (x)*
ACTA2	103.7	*MSX1*	49.4
ACTC1	111.4	*MYH7*	103.5
ACVRL1	60.4	*MYH9*	97.5
BRAF	160.0	*NF1*	190.7
CBL	192.3	*NIPBL*	175.9
CDKL5	146.1	*NOTCH2*	153.4
CHD7	150.6	*NRAS*	254.1
COL11A1	160.5	*NRTN*	45.8
COL11A2	66.8	*NSD1*	160.1
COL1A1	47.2	*OTX2*	115.1
COL1A2	127.0	*PHOX2B*	19.2
COL2A1	76.2	*PKHD1*	173.6
COL3A1	123.1	*PLOD1*	68.3
COL5A1	52.0	*PSPN*	66.5
COL5A2	159.2	*PTCH1*	111.0
COL9A1	147.4	*PTPN11*	152.6
COL9A2	52.4	*RAD21*	198.5
COMP	55.3	*RAF1*	154.9
CREBBP	50.1	*RASA1*	171.7
CUL7	68.8	*RET*	97.4
DCC	188.4	*RUNX2*	144.5
DDX3X	118.1	*SALL1*	91.7
ECE1	80.6	*SALL4*	93.8
EDN3	64.6	*SCN1B*	69.3
EDNRB	178.9	*SHH*	50.3
EFNB1	47.8	*SHOC2*	195.5
ENG	36.4	*SIX3*	80.0
EP300	191.0	*SIX6*	67.6
FBN1	177.2	*SMC1A*	134.7
FBN2	171.0	*SMC3*	157.2
FGFR1	102.7	*SOS1*	180.5
FGFR2	157.5	*SOX10*	45.1
FGFR3	34.8	*SOX2-OT*	89.0
GDNF	200.5	*SPRED1*	137.0
GFRA1	103.1	*SPRY2*	141.7
GFRA2	49.9	*STAG1*	193.3
GLA	121.1	*TAZ*	45.1
HRAS	44.4	*TBX22*	117.7
IHH	73.4	*TBX5*	124.2
IRF6	128.5	*TCF4*	170.8
JAG1	147.5	*TCOF1*	68.4
KCNE1	88.4	*TGFBR1*	190.0
KCNJ2	226.4	*TGFBR2*	89.6
KCNQ1	80.5	*TGIF1*	77.1
KIAA1279	186.5	*TP63*	182.5
KIF26A	33.7	*TRAPPC10*	139.7
KRAS	214.4	*TRIM37*	85.4
L1CAM	42.7	*TSC1*	157.8
LAMP2	128.2	*TSC2*	49.4
MAP2K1	151.4	*TWIST1*	47.9
MAP2K2	35.6	*VHL*	84.5
MAPK1	168.5	*VSX2*	29.7
MAPK3	87.1	*ZEB2*	218.9
MECP2	80.4	*ZIC2*	72.9
MID1	126.4		

according to reverse transcription (RT)-PCR studies, together with seven nonsynonymous substitutions (Table 5). Among the seven nonsynonymous substitutions, four were previously reported to be pathogenic based on functional assays or the inheritance pattern within the families (Li *et al.*, 1992; Fahsold *et al.*, 2000; Lee *et al.*, 2006).

Three samples with missense mutations that have never been reported in the literature were predicted to be pathogenic based on the consensus predication from multiple bioinformatics programs. Five programs, including SIFT, Polyphen2, LRT, Mutation Taster, and PhyloP, predicted potential pathogenicity as follows: c.2183T>G (p.Val728Gly) mutation was predicted to be pathogenic by all five programs, and c.2540T>G (p.Leu847Arg) and c.6818A>T (p.Lys2273Met) mutations were predicted to be pathogenic by four of the five bioinformatics programs. None of the three missense mutations resided within the critical functional domain, GAP-related domain that regulates the RasGAP activity.

Comparison of the distributions of nonsense, splice-site variants, and missense mutations in the Japanese population versus the northern European population, as reported by Messiaen *et al.* (2000), Nemethova *et al.* (2013), Sabbagh *et al.* (2013), and Valero *et al.* (2011), revealed no statistically significant differences among the groups ($p=0.203$ using the Fisher exact test for countable data).

Together with these 3 samples, which were subject to bioinformatics programs, 16 samples without truncating mutations or missense mutations, previously reported to be pathogenic, were further sequenced using direct capillary sequencing methods. All the exons were sequenced, including exon 1, and no additional point mutations or small indels were detected. These 19 patients were further screened for relatively large deletions that would span an entire exon or multiple exons and thus escape from direct capillary sequencing. Among 10 patients, 5 were shown to have a whole *NF1* deletion, 2 had multiple-exon deletions, and 3 had single-exon deletions. These five patients with a whole *NF1* deletion were apparently homozygous for all the SNPs for the entire *NF1* region according to the next-generation sequencing analysis.

Overall, no appreciable genotype–phenotype correlation was detected in the present study (Table 5). Variants were detected in genes other than *NF1* when the same criteria used in the *NF1* analysis were applied to these genes (Table 5). None of these variants was classified as truncating mutations and none of them listed in the Human Genome Mutation Database (HGMD) (Cooper *et al.*, 1998). Such rare variants of unknown significance among the genes on the panel were found in at least two-thirds of the patients. Patients with variants in genes other than *NF1* did not necessarily exhibit a severe *NF1* phenotype.

Discussion

The present study demonstrated that next-generation sequencing with in-solution hybridization-based enrichment provides a high mutation detection rate comparable to that of conventional direct capillary sequencing methods for the molecular diagnosis of neurofibromatosis. The overall mutation detection rate using the currently reported method in 86 patients who met the clinical diagnostic criteria was 81.4% (70/86). Among the 16 samples in which mutations were not detected using next-generation sequencing, 10 samples were later shown to have large deletions using a different method, multiplex ligation-dependent probe amplification (MLPA). Because of their large sizes, the 10 large deletions would not have been detected using the direct capillary sequencing

TABLE 5. SUMMARY OF PATHOGENIC MUTATIONS DETECTED BY NEXT-GENERATION SEQUENCING

Exon	*Genomic mutation*	*Amino acid substitution*	*Type of mutation*	*Reference*	*Age*	*Familial*	*Symptoms*	*Variations of unknown significance in rasopathy genes*	*Number of mutations in other genes*
2	c.83_84insG	p.Asn29Glufs*9	Frameshift		68	Yes	P,N	RASA1 c.293C>T p.Ala98Val	2
3	c.264_265insA	p.Thr89Asnfs*18	Frameshift		44	Yes	P,B,N		1
5	c.491T>A	p.Leu164*	Nonsense		50	Yes	P,B,O,N		1
5	c.495-498delTGTT	p.Cys167Glnfs*10	Frameshift		41	No	P,N,L		1
5	c.499_500insG	p.Cys167Trpfs*7	Frameshift		27	No	P,B,N,L		1
5	c.574C>T	p.Arg192*	Nonsense		32	No	P,N,L		2
10	c.1105C>T	p.Gln369*	Nonsense		40	Yes	P,N,L		1
11	c.1241T>G	p.Leu414Arg	Missense[a]	Lee *et al.* (2006)	21	No	P,N,L		1
11	c.1246C>T	p.Arg416*	Nonsense		32	Yes	P,B,N		1
12	c.1381C>T	p.Arg461*	Nonsense		3	No	P	RASA1 c.669G>C p.Gln223His	1
12	c.1381C>T	p.Arg461*	Nonsense		67	Yes	P,B,N		1
12	c.1381C>T	p.Arg461*	Nonsense		41	Yes	P,B,N		0
13	c.1466A>G	p.Tyr489Cys	Missense[a]	Messiaen *et al.* (2000)	36	No	P,N		1
13	c.1466A>G	p.Tyr489Cys	Missense[a]	Messiaen *et al.* (2000)	63	Yes	P,B,N		0
13	c.1466A>G	p.Tyr489Cys	Missense[a]	Messiaen *et al.* (2000)	71	No	P,N,L		1
13	c.1527+1_+4delGTAA		Splicing		30	No	P,N,L		2
14	c.1541_1542delAG	p.Gln514Argfs*43	Frameshift		52	No	P,B,N		1
15	c.1721+3A>G		Splicing	Purandare *et al.* (1994)	40	Yes	P,B,N		0
16	c.1726C>T	p.Gln576*	Nonsense		36	No	P,N		0
16	c.1754_1757delACTA	p.Thr586Valfs*18	Frameshift		49	Yes	P,N		0
16	c.1765C<T	p.Gln589*	Nonsense		40	No	P,N		1
16	c.1832delT	p.Asn614Ilefs*17	Frameshift		80	No	P,N,L		3
17	c.1876_1877insT	p.Tyr628Leufs*6	Frameshift		79	Yes	P,B,N,L		2
17	c.1885G>A	p.Gly629Arg	Missense[a]	Gasparini *et al.* (1996)	57	Yes	P,N		2
18	c.2041C>T	p.Arg681*	Nonsense		23	No	P,N		1
18	c.2041C>T	p.Arg681*	Nonsense		35	Yes	P,B,N		1
18	c.2087G>A	p.Trp696*	Nonsense		58	Yes	P,B,N,L		0
18[b]	c.2183T>G	p.Val728Gly	Missense		67	Yes	P,N		0
21	c.2423delT	p.His809Thrfs*12	Frameshift		43	Yes	P,N		1
21	c.2540T>C	p.Leu847Pro	Missense[a]	Fahsold *et al.* (2000)	33	Yes	P,N,L		0
21	c.2540T>C	p.Leu847Pro	Missense[a]	Fahsold *et al.* (2000)	59	Yes	P,B,N,L		0

(*continued*)

TABLE 5. (CONTINUED)

Exon	*Genomic mutation*	*Amino acid substitution*	*Type of mutation*	*Reference*	*Age*	*Familial*	*Symptoms*	*Variations of unknown significance in rasopathy genes*	*Number of mutations in other genes*
21[b]	c.2540T>G	p.Leu847Arg	Missense		55	No	P,N		0
21	c.2446C>T	p.Arg816*	Nonsense		52	Yes	P,N,L		0
22	c.2851-5_-2delTTTA		Splicing		19	No	P,B,N,L		1
23	c.3048T>A	p.Cys1016*	Nonsense		50	Yes	P,B,N		0
24	c.3132C>A	p.Tyr1044*	Nonsense		12	Yes	P,O,N		0
25	c.3213_3214delAA	p.Ser1072Hisfs*16	Frameshift		29	No	P,N,L		2
27	c.3595_3596insGG	p.Thr1199Argfs*17	Frameshift		20	No	P,N,L		1
27	c.3615_3616delTG	p.Phe1205Leufs*12	Frameshift		37	Yes	P,B,N		2
27	c.3615_3616delTG	p.Phe1205Leufs*12	Frameshift		64	Yes	P,B,N,L		1
28	c.3709-2A>G		Splicing		44	No	P,B,N,L		0
28	c.3765_3766insCT	p.Leu1257Cysfs*10	Frameshift		29	No	P,B,N,L		2
28	c.3826C>T	p.Arg1276*	Nonsense		21	No	P,O,B,N,L		0
29	c.3888T>A	p.Tyr1296*	Nonsense		49	No	P,N,L		0
30	c.4084C>T	p.Arg1362*	Nonsense		27	No	P,N		1
32	c.4329delA	p.Lys1444Argfs*25	Frameshift		50	Yes	P,B,N,L		0
32	c.4330A>G	p.Lys1440Glu	Missense[a]	Li *et al.* (1992)	40	No	P,N,L		0
33	c.4430+1G>A		Splicing		49	Yes	P,B,N		2
34	c.4544delA	p.Gln1515Argfs*59	Frameshift		35	Yes	P,N		2
35	c.4716_4724+6 delTATGACTAGGTAAAG		Splicing		50	No	P,B,N,L		1
36	c.4743_4744delAG	p.Glu1582Argfs*39	Frameshift		36	No	P,B,N,L		2
36	c.4769T>G	p.Leu1590*	Nonsense		45	No	P,N		1
37	c.4873_4874insA	p.Tyr1625*	Nonsense		63	No	P,B,N		1
37	c.5198T>G	p.Leu1733*	Nonsense		40	No	P,B,N,L		1
38	c.5269-6_5276 delTTCCAGGTTGGTTC		Splicing		38	No	P,N,L		1
38	c.5269-1G>A		Splicing		39	Yes	P,B,N,L		0
38	c.5516_5517insC	p.Glu1841Profs*21	Frameshift		31	Yes	P,B,N		1
38	c.5609G>A	p.Arg1870Gln	Missense[a]	Ars *et al.* (2003)	69	Yes	P,B,N		0
40	c.5902C>T	p.Arg1968*	Nonsense		22	No	P,N		1
44	c.6675G>A	p.Trp2225*	Nonsense		54	No	P,O,B,N		3
45	c.6772C>T	p.Arg2258*	Nonsense		69	Yes	P,N		0
45	c.6772C>T	p.Arg2258*	Nonsense		52	Yes	P,B,N,L		1
45[b]	c.6818A>T	p.Lys2273Met	Missense		46	No	P,N		1

(*continued*)

TABLE 5. (CONTINUED)

Exon	*Genomic mutation*	*Amino acid substitution*	*Type of mutation*	*Reference*	*Age*	*Familial*	*Symptoms*	*Variations of unknown significance in rasopathy genes*	*Number of mutations in other genes*
46	c.6850_6853delACTT	p.Tyr2285Thrfs*5	Frameshift		42	Yes	P,N		1
46	c.6853_6854insA	p.Tyr2285*	Nonsense		21	No	P,N		0
46	c.6853_6854insA	p.Tyr2285*	Nonsense		28	No	P,N		0
46	c.6904C>T	p.Gln2302*	Nonsense		37	Yes	P,N,L		1
47	c.6950G>A	p.Trp2317*	Nonsense		25	No	P,B,N,L		0
50	c.7348C>T	p.Arg2450*	Nonsense		46	No	P,B,N,L		0
54	c.7970+1_+4delGTAA		Splicing		41	Yes	P,N,L		2
			ex1 to 58 deletion		13	No	P,N,L		3
			ex1 to 58 deletion		29	No	P,N		1
			ex1 to 58 deletion		68	No	P,N		1
			ex1 to 58 deletion		58	No	P,B,N,L		1
			ex1 to 58 deletion		34	No	P,B,N		1
			ex1 deletion		68	No	P,N,L		1
			ex3 to 4 deletion		59	No	P,N,L		0
			ex6 to 51 deletion		36	Yes	P,N,L		2
			ex8 deletion		28	Yes	P,N		0
			ex12 deletion		55	No	P,N		1
					37	No	P		0
					50	No	P,N		0
					45	Yes	P,N,L		2
					30	No	P,N		0
					34	Yes	P,B,N		1
					25	No	P		0

[a]Previously reported to cause aberrant splicing.
[b]Predicted to be pathogenic by bioinformatics programs.
Symptoms: P, pigment; O, optic nerve tumor; B, bone manifestation; N, neurofibroma; L, Lisch nodules; HGMD; Human Genome Mutation Database.

method, which is currently considered to be the gold standard. The mutation detection rate was 92.1% (70/76) when these 10 samples were excluded from the calculation of the detection rate.

Among the 10 samples with large deletions, 5 patients with a whole *NF1* deletion could have been suspected of having a whole gene deletion, in that these patients were apparently homozygous for all the SNPs for the entire *NF1* region according to the next-generation sequencing data. The remaining five patients with a partial deletion of the *NF1* gene, as documented using MLPA, would not have been reliably inferred to have such a deletion based on the relatively short runs of homozygosity.

Recent reports on comprehensive *NF1* screening using the direct capillary sequencing method revealed that the detection rate was 89.5–96.3% when cases with large deletions detectable only by using MLPA were excluded [93.4%: Valero *et al.* (2011), 89.5%: Nemethova *et al.* (2013), 96.3%: Sabbagh *et al.* (2013)]. Hence, the performance of the presently reported protocol was comparable with that of the direct capillary sequencing methods.

The present protocol uses genomic DNA as the starting material, unlike other protocols using puromycin-tested Epstein-Barr virus cell lines as the starting material for RT-PCR (Messiaen *et al.*, 2000). Apparently, the use of genomic DNA is much easier in clinical settings. Yet, genetic testing based on genomic DNA, including the previously reported protocol, cannot predict potential splicing defects caused by point mutations. The use of RNA would be more sensitive to splicing abnormalities, if any, because of the possibility of mutations located deep in the intron or aberrant splicing defects caused by point mutations within coding sequences that were not evaluated in the presently reported protocol. However, such deep intronic mutations or splicing defects may be relatively rare, given the high overall detection rate of 92.1% in the present study.

The mean coverage of the entire target regions per sample was 131.0x. This coverage figure was considered to be sufficient for the detection of heterozygous base changes. Furthermore, the observation that rare variants in some genes on the panel were found in at least two-thirds of the patients supports the notion that the diagnostic performance of the panel for other genes is as robust as it is for *NF1*. Thus, our results regarding the validity of next-generation sequencing for the molecular diagnosis of the *NF1* gene, in comparison with direct capillary sequencing, can be extrapolated to the molecular diagnosis of other classic malformation syndromes.

Nevertheless, exon-to-exon variations in the coverage figures should be carefully evaluated. The extremely low coverage of the *NF1* exon1 can be ascribed to its extremely high GC content of 77.5%, in that a GC content of 60% or higher is associated with a sharp decrease in the read depth (Chilamakuri *et al.*, 2014). Similarly, a relatively low coverage of the *COMP* gene of 55.3x may be associated with a GC content of 63.4%. Exon 15 and exon 50 of *NF1*, together with the *PHOX2B* gene, had relatively low coverages of 86.9x, 79.1x, and 19.2x, respectively. The underlying cause of such variations is currently unexplained in that the GC contents of these regions were 32.2%, 39.4%, and 54.5%, respectively.

We estimated that the cost for consumables would be about USD 400 for direct capillary sequencing of the *NF1* gene, excluding labor costs. The estimated cost for consumables for the NGS panel analysis would be comparable. Hence, if we were to screen for the single *NF1* gene, the cost–benefit of next-generation sequencing may not be advantageous. However, if we were to screen for genes associated with conditions to be differentiated from neurofibromatosis using direct capillary sequencing, the consumable cost would be multiplied, whereas the cost for the screening of extra genes using next-generation sequencing would remain fixed. Indeed, the molecular diagnosis of Legius syndrome and Noonan syndrome would be helpful for the clinical management and outcome predictions of patients with café-au-lait spots, since patients with these conditions are unlikely to develop neurofibromas or other hamartomatous complications.

The availability of a mutation analysis panel, like the one presented herein, plays a critical role in differentiating the underlying genetic cause of patients whose diagnosis is uncertain from a clinical standpoint (Takenouchi *et al.*, 2013a, 2013b). The use of a whole-exome panel would be advantageous because of its comprehensiveness. However, apart from the higher cost of a whole-exome analysis, a panel approach enables a higher sensitivity (Chin *et al.*, 2013) because the average coverage, and thus the sensitivity, is higher using a panel approach (close to 100%) compared with a whole-exome approach (85%–95%).

Acknowledgments

All the authors would like to express their sincere appreciation to Mr. Yuji Sugie for his special support and all the patients and their families who were enrolled in this study. This work was partly supported by Research on Applying Health Technology and Research on Rare and Intractable Diseases from the Ministry of Health, Labour and Welfare, Japan.

Author Disclosure Statement

The authors declare that they have no competing interests.

References

Abernathy CR, Rasmussen SA, Stalker HJ, *et al.* (1997) *NF1* mutation analysis using a combined heteroduplex/SSCP approach. Hum Mutat 9:548–554.

Adzhubei IA, Schmidt S, Peshkin L, *et al.* (2010) A method and server for predicting damaging missense mutations. Nat Methods 7:248–249.

Aoki Y, Niihori T, Narumi Y, *et al.* (2008) The RAS/MAPK syndromes: novel roles of the RAS pathway in human genetic disorders. Hum Mutat 29:992–1006.

Aramaki M, Udaka T, Torii C, *et al.* (2006) Screening for CHARGE syndrome mutations in the *CHD7* gene using denaturing high-performance liquid chromatography. Genet Test Mol Biomarkers 10:244–251.

Ars E, Kruyer H, Morell M, *et al.* (2003) Recurrent mutations in the *NF1* gene are common among neurofibromatosis type 1 patients. J Med Genet 40:e82.

Bausch B, Borozdin W, Mautner VF, *et al.* (2007) Germline *NF1* mutational spectra and loss-of-heterozygosity analyses in patients with pheochromocytoma and neurofibromatosis type 1. J Clin Endocrinol Metab 92:2784–2792.

Carey JC, Viskochil DH (1999) Neurofibromatosis type 1: A model condition for the study of the molecular basis of variable expressivity in human disorders. Am J Med Genet 89:7–13.